

# Biomolecular stabilisation near the unstable equilibrium of a biological system

Christian Cuba Samaniego<sup>1</sup>, Nicholas A. Delateur<sup>2</sup>, Giulia Giordano<sup>3</sup>, and Elisa Franco<sup>4</sup>

**Abstract**— We describe an approach to stabilize a bistable biological system near its unstable equilibrium using a molecular feedback controller. As a case study we focus on the classical toggle switch by Gardner and Collins. The controller relies on two parallel sequestration motifs, which yield two control species influencing the production rates of the toggle switch proteins. We show that the controller reshapes the equilibrium landscape to a single equilibrium. With numerical simulations we illustrate the effectiveness of our approach in stabilizing the closed-loop system around this unique equilibrium, which falls in a neighborhood of the toggle switch unstable equilibrium, if the controller parameters are properly tuned.

## I. INTRODUCTION

Bistable systems are very common in biology. Bistability is found, for example, in metabolic networks [1], in cellular processes such as division and differentiation [2], [3], and in cellular communities [4]. Bistability means that the system commits to either of two stable states, restricting the range of possible responses to environmental stimuli, and in this sense it can be seen as a source of robustness. However, there are cases in which bistability may be undesirable: tumor growth, for instance, can be promoted by a switch to a high energy metabolism [5]; in microbial consortia, a particular strain may cause a population-level switch and take over another, more beneficial microorganism [4].

Advances in synthetic biology and molecular programming have made it possible to build artificial systems with biomolecules (DNA, RNA and proteins) presenting rationally designed interactions. This includes *kinetic interactions*, opening up many opportunities to build arbitrary biochemical dynamical systems, including molecular feedback controllers [6], [7]. Building on these advances, we examine the problem of controlling the behavior of a bistable system using a reaction network that operates as a biomolecular controller, and makes it possible to tune the dynamic and steady state behavior of the bistable process without requiring its direct redesign.

<sup>1</sup>Biodesign Center for Biocomputing, Security & Society at Arizona State University, and Department of Biological Engineering at Massachusetts Institute of Technology. ccubasam@mit.edu. CC was supported by the CDMRP Breast Cancer Research Program Award BC132057.

<sup>2</sup>Department of Chemistry at Massachusetts Institute of Technology. delateur@mit.edu

<sup>3</sup>Delft Center for Systems and Control, Delft University of Technology, 2628 CD Delft, The Netherlands. g.giordano@tudelft.nl. GG was supported by the DTF grant at TU Delft and by the Dutch Research Council through the NWO Talent Scheme grant VI.Veni.192.035.

<sup>4</sup>Department of Mechanical and Aerospace Engineering, University of California Los Angeles, California 90095, USA. efranco@seas.ucla.edu

We consider the well known Gardner and Collins toggle switch as a simple test case [8]. We use a molecular controller that relies on two parallel layers of sequestration reactions [9], [10]. The controller senses the concentration of one of the species of the bistable switch, and produces two control outputs that influence both species of the toggle switch. Sequestration reactions are known to be an effective approach to build molecular controllers [11], [12], [7], [6]. Each sequestration layer of the controller described here is similar to the antithetic integral controller proposed in [13]; we include degradation of each participating species, and each sequestration layer provides a control output.

In Section II, we describe our general approach and provide relevant background. Section III reports our main results. Our simulation methods and parameters are in Section IV, and a brief discussion is in Section V.

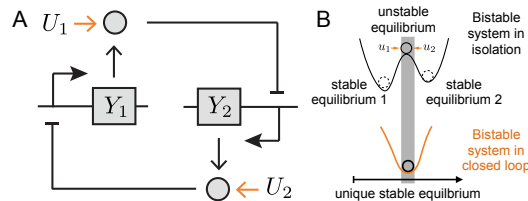


Fig. 1. A. We demonstrate regulation of a canonical bistable gene network to operate near its unstable equilibrium by using a molecular controller that provides two inputs  $U_1$  and  $U_2$ . B. By introducing a molecular controller, we force the equilibrium landscape of the closed loop system to present a single, stable equilibrium in a neighborhood of the unstable equilibrium of the toggle switch in isolation.

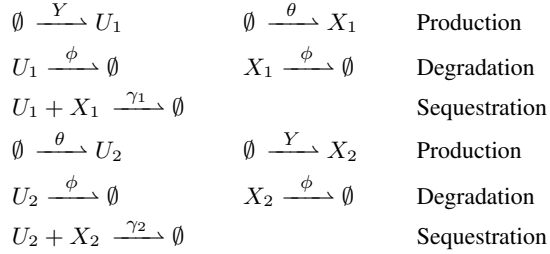
## II. APPROACH AND BACKGROUND

Fig. 1 A illustrates our approach to control the behavior of a bistable process. In our molecular bistable system, as usual, an unstable equilibrium is sandwiched between two stable equilibria. By introducing a controller, consisting of two control inputs with opposite effects on the state of the system, we would like to induce a stabilization of the unstable equilibrium. In practice, however, we will show that if the controller parameters are chosen appropriately, the *closed loop system* can undergo a transformation of the equilibrium landscape and can transition to a single, stable equilibrium point, as sketched in Fig. 1 B. Thus, by adding a molecular control loop we can radically transform the behavior of the process, without directly engineering the process itself. This may be important in applications in which genetically modifying a bistable process may be challenging or impossible due to its complexity, or in which mutating promoters may cause unknown perturbations to the host. In

the rest of this paper, we indicate molecular species with capital letters, and their concentration with the corresponding lowercase letter.

### A. Parallel modules for molecular sequestration

Each molecular sequestration module consists of two species  $U_i$  and  $X_i$ , which mutually sequester with rate constant  $\gamma_i$ ,  $i = 1, 2$ , forming a waste complex. The modules are illustrated in Fig. 2. In the first module, species  $X_1$  is produced at a constant rate  $\theta$ ; in the second module,  $U_2$  is produced from an input species  $Y$ , with unitary reaction rate constant for illustrative purposes. In the second module, species  $X_2$  is produced from the input species  $Y$  with a unitary reaction rate constant, while  $U_2$  is produced at a constant rate  $\theta$ . We assume, for simplicity, that all species are degraded at the same rate  $\phi$ . The list of chemical reactions describing the two modules is:



Using the law of mass action, we can write the corresponding Ordinary Differential Equations (ODEs):

$$\dot{u}_1 = y - \gamma_1 u_1 x_1 - \phi u_1, \quad (1)$$

$$\dot{x}_1 = \theta - \gamma_1 u_1 x_1 - \phi x_1, \quad (2)$$

$$\dot{u}_2 = \theta - \gamma_2 u_2 x_2 - \phi u_2, \quad (3)$$

$$\dot{x}_2 = y - \gamma_2 u_2 x_2 - \phi x_2. \quad (4)$$

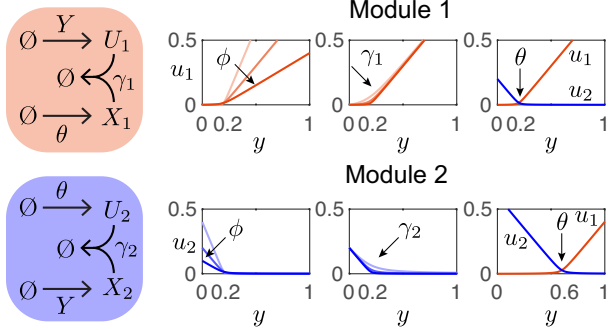


Fig. 2. Simulations examining the performance of a two-layer molecular controller based on sequestration. Left: schematic of the controller modules described in Equations (1)-(2). Right: Sensitivity analysis of the input-output map of each controller module, when a single parameter is varied. Orange lines correspond to  $u_1$  (the output of Module 1), and blue lines correspond to  $u_2$  (the output of Module 2). Ultrasensitivity of the response can be improved when  $\phi_i$  is small, and  $\gamma_i$  is large,  $i = 1, 2$ . The threshold of the controller response is determined by  $\theta$ , which has an “opposite” effect on the output of each module.

Molecular sequestration in each module generates an ultrasensitive input-output map with a tunable threshold if the sequestration rates  $\gamma_i$ ,  $i = 1, 2$  are sufficiently fast [14]. When the concentration of species  $U_1$  is larger than the

concentration of species  $X_1$ , then  $X_1$  should be completely sequestered, while  $U_1$  is still available for downstream (slower) reactions; conversely, if the concentration of  $X_1$  is larger than that of  $U_1$ , all  $U_1$  is sequestered allowing only  $X_1$  to participate in other reactions (Fig. 2). Overall, the less abundant species defines the tunable threshold [14]. Next, we derive approximated steady-state expressions that describe the input-output map of the modules.

1) *Steady state analysis of the parallel molecular sequestration modules:* Next, we aim to find expressions for the steady states  $\bar{u}_1$  and  $\bar{u}_2$  as a function of a constant input concentration  $\bar{y}$ . To do this, we set Equations (1) and (2) equal to zero ( $\dot{u}_1 = \dot{x}_1 = 0$ ), and we find:

$$\bar{x}_1 = \frac{y - \phi \bar{u}_1}{\gamma_1 \bar{u}_1} = \frac{\theta}{\gamma_1 \bar{u}_1 + \phi},$$

The value of  $\bar{u}_1$  can be computed by finding the roots of a second order polynomial equation  $a_1 \bar{u}_1^2 + b_1 \bar{u}_1 + c_1 = 0$ , where  $a_1 = 1$ ,  $b_1 = \phi/\gamma_1 + (\theta - y)/\phi$  and  $c_1 = -y/\gamma_1$ . The constant term  $c_1$  is always negative, resulting in a single positive solution,  $\bar{u}_1 = \frac{1}{2a_1} \left( -b_1 + \sqrt{b_1^2 - 4a_1 c_1} \right)$ . If  $\gamma_1$  is very large ( $\gamma_1 \gg 1$ ,  $\gamma_1 \gg \phi$ ), then  $c_1 \approx 0$  and  $b_1 \approx (\theta - y)/\phi$ , hence the solution can be approximated as:

$$\bar{u}_1(y) \approx \frac{|b_1| - b_1}{2} = \begin{cases} 0 & \text{if } y < \theta \\ (y - \theta)/\phi & \text{if } y \geq \theta \end{cases} \quad (5)$$

Following similar steps, we set Equations (3) and (4) equal to zero ( $\dot{u}_2 = \dot{x}_2 = 0$ ), and find

$$\bar{x}_2 = \frac{\theta - \phi \bar{u}_2}{\gamma_2 \bar{u}_2} = \frac{y}{\gamma_2 \bar{u}_2 + \phi}.$$

The steady state  $\bar{u}_2$  can be found by finding the roots of the second order polynomial equation  $a_2 \bar{u}_2^2 + b_2 \bar{u}_2 + c_2 = 0$ , where  $a_2 = 1$ ,  $b_2 = \phi/\gamma_2 + (y - \theta)/\phi$  and  $c_2 = -\theta/\gamma_2$ . The constant term  $c_2$  is always negative, resulting in a single positive solution,  $\bar{u}_2 = \frac{1}{2a_2} \left( -b_2 + \sqrt{b_2^2 - 4a_2 c_2} \right)$ . If  $\gamma_2 \gg \theta$  and  $\gamma_2 \gg \phi$ , then  $c_2 \approx 0$  and  $b_2 \approx (y - \theta)/\phi$ , hence the solution can be approximated as:

$$\bar{u}_2(y) \approx \frac{|b_2| - b_2}{2} = \begin{cases} (\theta - y)/\phi & \text{if } y \leq \theta \\ 0 & \text{if } y > \theta \end{cases} \quad (6)$$

Overall, the approximated expressions (5) and (6) highlight that the controller output is either very small or proportional to the difference between  $y$  and  $\theta$  when the input  $y$  exceeds (first module) or is below (second module) the threshold  $\theta$ . Simulations illustrating the steady state response of the controller modules are in Fig. 2, right (simulation parameters are in Table II). The modules present an “opposite” output trend with respect to the threshold  $\theta$ .

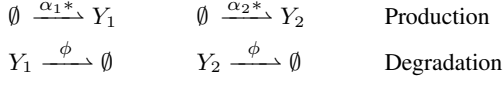
When  $y = \theta$ , the exact expression of  $u_i$  (without introducing approximations) is

$$u_i(\theta) = \frac{-\phi/\gamma_i + \sqrt{(\phi/\gamma_i)^2 + 4\theta/\gamma_i}}{2}$$

and it is apparent that, in the limit of  $\gamma_i \rightarrow \infty$ ,  $u_i(\theta) \rightarrow 0$ .

### B. The Gardner and Collins toggle switch

For the reader's convenience, we shortly describe the well-known Gardner and Collins' toggle switch [8]. It consists of two species  $Y_1$  and  $Y_2$  that repress each other. A Hill function describes the repression kinetics, with a maximum production rate  $\alpha_1$  and  $\alpha_2$ , a dissociation constant  $\kappa_1$  and  $\kappa_2$ , and Hill exponent  $n$ .



where  $\alpha_1^* = \alpha_1 \frac{\kappa_2^n}{\kappa_2^n + y_2^n}$  and  $\alpha_2^* = \alpha_2 \frac{\kappa_1^n}{\kappa_1^n + y_1^n}$ . Using the law of mass action we can write the ODEs:

$$\dot{y}_1 = \alpha_1 \frac{\kappa_2^n}{\kappa_2^n + y_2^n} - \phi y_1 \quad (7)$$

$$\dot{y}_2 = \alpha_2 \frac{\kappa_1^n}{\kappa_1^n + y_1^n} - \phi y_2 \quad (8)$$

These equations can be normalized by defining  $\hat{y}_1 = y_1/\kappa_1$ ,  $\hat{y}_2 = y_2/\kappa_2$ ,  $\hat{\alpha}_1 = \alpha_1/(\kappa_1\phi)$ ,  $\hat{\alpha}_2 = \alpha_2/(\kappa_2\phi)$ , and rescaling time as  $\tau = \phi t$ :

$$\frac{d\hat{y}_1}{d\tau} = \alpha_1 \frac{1}{1 + \hat{y}_2^n} - \hat{y}_1 \quad (9)$$

$$\frac{d\hat{y}_2}{d\tau} = \alpha_2 \frac{1}{1 + \hat{y}_1^n} - \hat{y}_2 \quad (10)$$

The steady states of these equations are:

$$\tilde{y}_1 = \frac{\hat{\alpha}_1}{1 + \tilde{y}_2^n}, \quad \tilde{y}_2 = \frac{\hat{\alpha}_2}{1 + \tilde{y}_1^n}$$

In the rest of this paper we assume that the parameters of the toggle switch are chosen to guarantee bistability. When  $\hat{\alpha}_1 = \hat{\alpha}_2 = \hat{\alpha}$ , the condition for bistability [15] is

$$\hat{\alpha} > \sqrt[n]{\frac{n^n}{(n-1)^{n+1}}} \quad \text{for } n > 1$$

When  $\hat{\alpha}_1$  and  $\hat{\alpha}_2$  are different and  $n = 2$ , the condition for bistability [16] depends on a third order polynomial,

$$a_1 \hat{\alpha}_1^3 + a_2 \hat{\alpha}_1^2 + a_3 \hat{\alpha}_1 + a_4 < 0,$$

where  $a_1 = 256$ ,  $a_2 = -3(9\hat{\alpha}_2^2 + 32\hat{\alpha}_2 - 256)$ ,  $a_3 = -96(\hat{\alpha}_2^2 + 29\hat{\alpha}_2 - 8)$  and  $a_4 = 256(\hat{\alpha}_2 + 1)^3$ .

### III. STABILIZATION OF A TOGGLE SWITCH

We now describe the model for the closed loop system in which the toggle switch in Equations (7)-(8) is the process we want to control using two molecular sequestration modules, which are similar to those described in Equations (1)-(4). The architecture is sketched in Fig. 3.

From an implementation point of view, the controller species  $U_i$  and  $X_i$ ,  $i = 1, 2$  are expected to be RNA molecules, which can be designed to include domains for mutual sequestration as well as domains for translation. The controller output species, as before, are  $U_1$  and  $U_2$ ; these species produce respectively  $Y_1$  and  $Y_2$  at rate constants  $\beta_1$  and  $\beta_2$ ; this assumption is reasonable if the controller species are RNA molecules that are translated into proteins  $Y_1$  and

$Y_2$ . The production of  $U_1$  is repressed by  $Y_1$ , rather than being produced at a rate that is linear in  $Y_1$  as in the original model at Equation (1); this choice is convenient in practice, because  $Y_1$  operates as a repressor within the toggle switch, so naturally  $U_1$  could be regulated by the same promoter repressed by  $Y_1$ .  $U_1$  is also sequestered by the controller species  $X_1$ , which is produced at a constant *reference* rate  $\theta$ . The second module of the controller produces species  $U_2$  at a constant rate of  $\theta$ , while the production of  $X_2$  is repressed by  $Y_1$  (like in the case of  $U_1$ ); in addition, species  $U_2$  and  $X_2$  sequester each other. All the species decay at rate  $\phi$ .

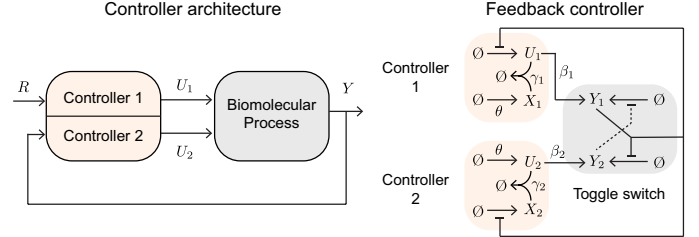


Fig. 3. Left: Architecture of the closed loop system that relies on two control species  $U_1$  and  $U_2$ . Right: More detailed schematic of the closed loop system.

The ODEs corresponding to the closed loop system are:

$$\dot{y}_1 = \alpha_1 \frac{\kappa_2^n}{\kappa_2^n + y_2^n} - \phi y_1 \quad \underbrace{+\beta_1 u_1}_{\text{Control input 1}} \quad (11)$$

$$\dot{y}_2 = \alpha_2 \frac{\kappa_1^n}{\kappa_1^n + y_1^n} - \phi y_2 \quad \underbrace{+\beta_2 u_2}_{\text{Control input 2}} \quad (12)$$

$$\dot{u}_1 = \alpha_2 \frac{\kappa_1^n}{\kappa_1^n + y_1^n} - \gamma_1 u_1 x_1 - \phi u_1 \quad (13)$$

$$\dot{x}_1 = \theta - \gamma_1 u_1 x_1 - \phi x_1 \quad (14)$$

$$\dot{u}_2 = \theta - \gamma_2 u_2 x_2 - \phi u_2 \quad (15)$$

$$\dot{x}_2 = \alpha_2 \frac{\kappa_1^n}{\kappa_1^n + y_1^n} - \gamma_2 u_2 x_2 - \phi x_2 \quad (16)$$

The model above can be made nondimensional by defining the following variables:  $\hat{y}_1 = y_1/\kappa_1$ ,  $\hat{y}_2 = y_2/\kappa_2$ ,  $\hat{\alpha}_1 = \alpha_1/(\kappa_1\phi)$ ,  $\hat{\alpha}_2 = \alpha_2/(\kappa_2\phi)$ ,  $\hat{\beta}_1 = \beta_1/(\kappa_1\phi)$ ,  $\hat{\beta}_2 = \beta_2/(\kappa_2\phi)$ ,  $\hat{\gamma}_1 = \gamma_1/\phi$ ,  $\hat{\gamma}_2 = \gamma_2/\phi$ ,  $\hat{\theta} = \theta/\phi$ , and  $\tau = \phi t$ . This leads to the ODE system:

$$\frac{d\hat{y}_1}{d\tau} = \frac{\hat{\alpha}_1}{1 + \hat{y}_2^n} - \hat{y}_1 + \hat{\beta}_1 u_1 \quad (17)$$

$$\frac{d\hat{y}_2}{d\tau} = \frac{\hat{\alpha}_2}{1 + \hat{y}_1^n} - \hat{y}_2 + \hat{\beta}_2 u_2 \quad (18)$$

$$\frac{du_1}{d\tau} = \frac{\hat{\alpha}_2}{1 + \hat{y}_1^n} - \hat{\gamma}_1 u_1 x_1 - u_1 \quad (19)$$

$$\frac{dx_1}{d\tau} = \hat{\theta} - \hat{\gamma}_1 u_1 x_1 - x_1 \quad (20)$$

$$\frac{du_2}{d\tau} = \hat{\theta} - \hat{\gamma}_2 u_2 x_2 - u_2 \quad (21)$$

$$\frac{dx_2}{d\tau} = \frac{\hat{\alpha}_2}{1 + \hat{y}_1^n} - \hat{\gamma}_2 u_2 x_2 - x_2 \quad (22)$$

In the rest of the paper we will work with the nondimensional model (17)–(22).

### A. Steady state analysis of the closed loop system

1) *The toggle switch with inputs admits one or three equilibria:* We restrict our attention to the toggle switch model that includes two additive inputs. We show that in the presence of bounded inputs, the toggle switch can present either one or three steady states. Starting from model (17)–(22), we focus on Equations (17)–(18) and we define  $u_i^* = \hat{\beta}_i u_i$ , obtaining the following ODES:

$$\frac{d\hat{y}_1}{d\tau} = \frac{\hat{\alpha}_1}{1 + \hat{y}_2^n} - \hat{y}_1 + u_1^* \quad (23)$$

$$\frac{d\hat{y}_2}{d\tau} = \frac{\hat{\alpha}_2}{1 + \hat{y}_1^n} - \hat{y}_2 + u_2^*. \quad (24)$$

The following proposition holds.

*Proposition 1:* System (23)–(24), in which  $n = 2$ , and  $u_i^*$ ,  $i = 1, 2$  are nonnegative bounded constants, admits either one or three equilibrium points.

*Proof:* The equilibria of system (23)–(24) are the solutions  $\tilde{y}_i$ ,  $i = 1, 2$  of the following equations:

$$\begin{cases} \tilde{y}_1 = u_1^* + \frac{\hat{\alpha}_1}{1 + \tilde{y}_2^n} \\ \tilde{y}_2 = u_2^* + \frac{\hat{\alpha}_2}{1 + \tilde{y}_1^n}. \end{cases} \quad (25)$$

We derive a polynomial equilibrium condition, whose only variable is  $\tilde{y}_1$ :

$$P(\tilde{y}_1) = a_5 \tilde{y}_1^5 - a_4 \tilde{y}_1^4 + a_3 \tilde{y}_1^3 - a_2 \tilde{y}_1^2 + a_1 \tilde{y}_1 - a_0 = 0,$$

in which  $a_5 = 1 + u_2^{*2}$ ,  $a_4 = \hat{\alpha}_1 + u_1^* + u_1^* u_2^{*2}$ ,  $a_3 = 2(1 + \hat{\alpha}_2 u_2^* + u_2^{*2})$ ,  $a_2 = 2(\hat{\alpha}_1 + u_1^* + \hat{\alpha}_2 u_1^* u_2^* + u_1^* u_2^{*2})$ ,  $a_1 = 1 + (\hat{\alpha}_2 + u_2^*)^2$ , and  $a_0 = \hat{\alpha}_1 + u_1^* + u_1^* (\hat{\alpha}_2 + u_2^*)^2$ . All coefficients  $\alpha_i$ ,  $i = 1, \dots, 5$  are positive, for arbitrary choices of the system reaction rate constants and parameters. First, since this is an odd-degree polynomial, it must have at least one real solution. Because  $P(-\tilde{y}_1)$  has no sign changes, the polynomial does not admit any negative real solution. Thus, the polynomial always admits at least one real positive solution. Using the Descartes rule, since there are 5 sign changes in the coefficients of  $P(\tilde{y}_1)$ , there can be at most 5 real positive solutions (they could be 5, 3, or 1). To quantify their number, we build the Routh Table I, in which we define:

$$\begin{aligned} b_1 &= \frac{a_4 a_3 - a_2 a_5}{a_4} = \frac{2\hat{\alpha}_1 \hat{\alpha}_2 u_2^*}{\hat{\alpha}_1 + u_1^* + u_1^* u_2^{*2}} > 0 \\ b_2 &= \frac{a_4 a_1 - a_0 a_5}{a_4} = \frac{\hat{\alpha}_1 \hat{\alpha}_2 (\hat{\alpha}_2 + 2u_2^*)}{\hat{\alpha}_1 + u_1^* + u_1^* u_2^{*2}} > 0 \\ c_1 &= \frac{a_4 b_2 - a_5 b_1}{b_1} \\ &= \frac{\hat{\alpha}_1 \hat{\alpha}_2 + \hat{\alpha}_2 u_1^* - 2\hat{\alpha}_1 u_2^* - 2u_1^* u_2^* - 3\hat{\alpha}_2 u_1^* u_2^{*2} - 2u_1^* u_2^{*3}}{2u_2^*} \\ d_1 &= \frac{c_1 b_2 + a_0 b_1}{c_1} = \frac{\hat{\alpha}_1 \hat{\alpha}_2^3}{2u_2^*} \left( \frac{1}{c_1} \right) \end{aligned}$$

Because  $c_1$  and  $d_1$  always have the same sign, the Routh table always has exactly 3 sign changes, hence there are always three solutions with positive real part. One must be real, and we know it is positive. The other two can be either real or complex. If they are real and positive, then the polynomial

has three positive real solutions, *i.e.* the system has three equilibria. If they are complex, then the polynomial has a single positive real solution, *i.e.* the system has a single equilibrium. The polynomial does not admit five positive real solutions. In conclusion, the system admits either one or three equilibria (corresponding to the real and positive solutions of the polynomial). ■

TABLE I  
ROUTH TABLE ASSOCIATED WITH THE POLYNOMIAL EQUILIBRIUM CONDITIONS FOR SYSTEM (23)–(24)

5	$a_5$	$a_3$	$a_1$
4	$-a_4$	$-a_2$	$-a_0$
3	$b_1$	$b_2$	0
2	$c_1$	$-a_0$	0
1	$d_1$	0	0
0	$-a_0$	0	0

### B. Stability analysis of the closed loop system

Here we demonstrate that by tuning the controller it is possible to force the closed loop system to have a unique, stable equilibrium.

1) *The controller tunes the equilibrium conditions of the closed loop system:* Here we illustrate how a suitable choice of the controller parameters can force the closed loop system to admit a single equilibrium. For this purpose, we first derive equilibrium conditions in the  $\tilde{y}_1, \tilde{y}_2$  plane and we show that they intersect at a single point if the controller is tuned properly.

We start by computing the equilibrium conditions by setting Equations (17) and (18) equal to zero. After some manipulation, this yields the two equations

$$\tilde{y}_2 = \sqrt[n]{\frac{\hat{\alpha}_1}{\tilde{y}_1 - \hat{\beta}_1 \tilde{u}_1(\tilde{y}_1)} - 1} \quad (26)$$

$$\tilde{y}_2 = \frac{\hat{\alpha}_2}{1 + \tilde{y}_1^n} + \hat{\beta}_2 \tilde{u}_2(\tilde{y}_1) \quad (27)$$

Next, we find  $\tilde{u}_1$  and  $\tilde{u}_2$  as a function of  $\tilde{y}_1$ ; we will follow the same steps taken to derive expressions (5) and (6).

We start with  $\tilde{u}_1(\tilde{y}_1)$ : we set Equations (19) and (20) equal to zero ( $\frac{du_1}{d\tau} = \frac{dx_1}{d\tau} = 0$ ), and we find:

$$\tilde{x}_1 = \frac{\hat{\alpha}_2(\tilde{y}_1) - \tilde{u}_1}{\hat{\gamma}_1 \tilde{u}_1} = \frac{\hat{\theta}}{\hat{\gamma}_1 \tilde{u}_1 + 1},$$

where  $\hat{\alpha}_2(\tilde{y}_1) = \hat{\alpha}_2 / (1 + \tilde{y}_1^n)$ . This results in a second order polynomial equation  $a_1 \tilde{u}_1^2 + b_1 \tilde{u}_1 + c_1 = 0$ , where  $a_1 = 1$ ,  $b_1 = 1/\hat{\gamma}_1 + \hat{\theta} - \hat{\alpha}_2(\tilde{y}_1)$  and  $c_1 = -\hat{\alpha}_2(\tilde{y}_1)/\hat{\gamma}_1$ . The constant term  $c_1$  is negative, resulting in a single positive solution,  $\tilde{u}_1 = \frac{1}{2a_1} \left( -b_1 + \sqrt{b_1^2 - 4c_1 a_1} \right)$ . If  $\hat{\gamma}_1$  is very large,  $c_1 \approx 0$  and  $b_1 \approx \hat{\theta} - \hat{\alpha}_2(\tilde{y}_1)$ , and the solution can be approximated as:

$$\tilde{u}_1(\tilde{y}_1) \approx \frac{|b_1| - b_1}{2} = \begin{cases} 0 & \text{if } \hat{\alpha}_2(\tilde{y}_1) < \hat{\theta} \\ \hat{\alpha}_2(\tilde{y}_1) - \hat{\theta} & \text{if } \hat{\alpha}_2(\tilde{y}_1) \geq \hat{\theta} \end{cases} \quad (28)$$

We look for  $\tilde{u}_2(\tilde{y}_1)$  by following similar steps. First, we set Equations (21) and (22) equal to zero ( $\frac{d\tilde{u}_2}{d\tau} = \frac{dx_2}{d\tau} = 0$ ), and we find

$$\tilde{x}_2 = \frac{\hat{\theta} - \tilde{u}_2}{\hat{\gamma}_2 \tilde{u}_2} = \frac{\hat{\alpha}_2(\tilde{y}_1)}{\hat{\gamma}_2 \tilde{u}_2 + 1},$$

where again  $\hat{\alpha}_2(\tilde{y}_1) = \hat{\alpha}_2/(1 + \tilde{y}_1^n)$ . This yields a second order polynomial  $a_2 \tilde{u}_2^2 + b_2 \tilde{u}_2 + c_2 = 0$ , where  $a_2 = 1$ ,  $b_2 = 1/\hat{\gamma}_2 + \hat{\alpha}_2(\tilde{y}_1) - \hat{\theta}$  and  $c_2 = -\hat{\theta}/\hat{\gamma}_2$ . The constant term  $c_2$  is negative, resulting in a single positive solution,  $\tilde{u}_2 = \frac{1}{2a_2} \left( -b_2 + \sqrt{b_2^2 - 4a_2c_2} \right)$ . If  $\hat{\gamma}_2$  is very large,  $c_2 \approx 0$  and  $b_2 \approx \hat{\alpha}_2(\tilde{y}_1) - \hat{\theta}$ , and the solution can be approximated as

$$\tilde{u}_2(\tilde{y}_1) \approx \frac{|b_2| - b_2}{2} = \begin{cases} \hat{\theta} - \hat{\alpha}_2(\tilde{y}_1) & \text{if } \hat{\alpha}_2(\tilde{y}_1) \leq \hat{\theta} \\ 0 & \text{if } \hat{\alpha}_2(\tilde{y}_1) > \hat{\theta}. \end{cases} \quad (29)$$

Going back to the equilibrium conditions (26) and (27), written at the beginning of this section, we can substitute the approximated expressions for the steady state controller variables  $\tilde{u}_1(\tilde{y}_1)$ , expression (28), and  $\tilde{u}_2(\tilde{y}_1)$ , expression (29).

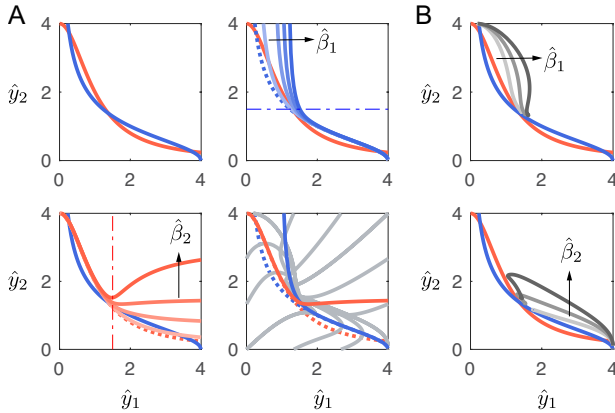


Fig. 4. Simulations illustrating the effects of the molecular controller on the closed loop equilibrium conditions; blue: condition (26), red: condition (27); gray: trajectories. A) Top left: Equilibrium conditions of the toggle switch in isolation, *i.e.* conditions (26) and (27) with  $\tilde{u}_1 = \tilde{u}_2 = 0$ . Top left and bottom right: closed loop equilibrium conditions when either  $\hat{\beta}_1$  or  $\hat{\beta}_2$  are varied. Dashed-dotted lines mark the controller threshold  $K_c$ . Bottom right: closed loop equilibrium conditions and overlapped trajectories that converge to the single equilibrium when using the nominal parameters (Table II); dashed lines correspond to the equilibrium conditions of the toggle switch in isolation, highlighting that the closed loop equilibrium is very close to the unstable equilibrium of the toggle, given the choice of controller threshold. B: Effects of increasing  $\hat{\beta}_i$  on the closed loop trajectories overlapped to the equilibrium conditions of the toggle switch in isolation.

In the case of a repressor dimer,  $n = 2$ , we define a threshold  $K_c = \sqrt{(\hat{\alpha}_2 - \hat{\theta})/\hat{\theta}}$ , and we note that  $\tilde{u}_1$  is positive only if  $\tilde{y}_1 \leq K_c$ , and is negligible if  $\tilde{y}_1$  exceeds the  $K_c$ . Note that the threshold  $K_c$  is determined by the value of  $\hat{\theta}$ , which is a reference parameter of the molecular controller. This means that the equilibrium condition (26) is identical to the equilibrium condition of the toggle switch in the absence of inputs when  $\tilde{y}_1$  exceeds the threshold  $K_c$ . The equilibrium condition is altered, relative to the no-input case, only if  $\tilde{y}_1$  is below the threshold  $K_c$ . Conversely,  $\tilde{u}_2$  is positive only when  $\tilde{y}_1 \geq K_c$ , and negligible when  $\tilde{y}_1 < K_c$ , thus the equilibrium condition (27) is identical to the no-input case

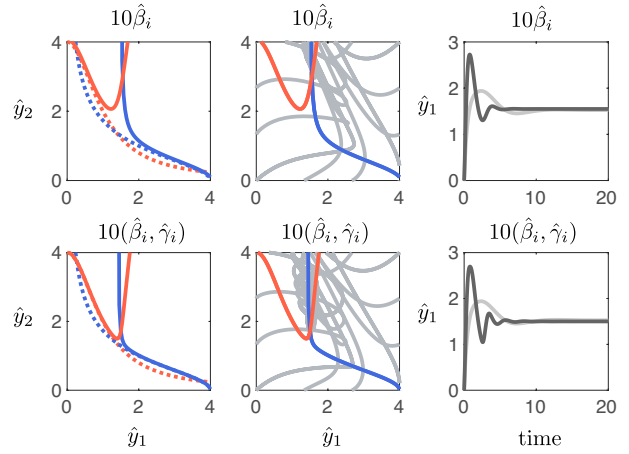


Fig. 5. Simulations illustrating the effects of an aggressive molecular controller on the closed loop equilibrium conditions. Left column, top: if  $\hat{\beta}_i$  are too large, the unique equilibrium becomes far from the unstable equilibrium of the toggle in isolation; bottom: by increasing  $\hat{\gamma}_i$  (sequestration rate constant), the controller ultrasensitivity improves (see Fig. 2) and the closed loop equilibrium becomes closer to the unstable equilibrium of the toggle switch. Center column: equilibrium conditions overlapped with a series of trajectories. Right column: Example solutions highlighting that for large  $\hat{\beta}_i$  the overshoot increases (light gray line corresponds to the solution with  $\hat{\beta}_i$  having its nominal value (Table II); dark gray line corresponds to  $10\hat{\beta}_i$  (top) or  $10\hat{\beta}_i, 10\hat{\gamma}_i$  (bottom).

when  $\tilde{y}_1 < K_c$ , and departs from the no-input condition only when  $\tilde{y}_1 \geq K_c$ .

We now focus on the case in which the Hill coefficient is  $n = 2$  (dimer repressors in the toggle switch). Proposition 1 ensures that when  $n = 2$  the closed loop system presents either one or three equilibria. This means that the equilibrium conditions (26) and (27) can have either one or three intersections. If the toggle switch in isolation does exhibit three equilibria (see Section II-B), then the equilibrium conditions (26) and (27) with  $\tilde{u}_1 = \tilde{u}_2 = 0$  (no-input case) must have three intersections. In the presence of a controller, then  $\tilde{u}_1$  and  $\tilde{u}_2$  may become non-zero, so the controller provides an opportunity to alter the shape of the equilibrium conditions in relation to the controller threshold  $K_c$ . The simplest tuning knob for the controller are the reaction rates  $\hat{\beta}_1$  and  $\hat{\beta}_2$ , which directly amplify the influence of the controller on the steady state expressions (26) and (27).

In Figs. 4 and 5 we illustrate the qualitative analysis above with numerical simulations. These simulations indicate that large  $\beta_i$  is beneficial to guarantee a single intersection in the equilibrium conditions, thus the presence of a single equilibrium which falls in a neighborhood of the unstable equilibrium of the toggle switch in isolation (Fig. 4 A) due to a suitable choice of the controller threshold. However, if  $\beta_i$  are too large, they cause an increase in the distance of the single closed loop equilibrium from the unstable equilibrium of the toggle switch in isolation, which may not be a desirable feature (Fig. 5, left column, top). This effect can be compensated by increasing the sequestration rates  $\gamma_i$ , because they improve ultrasensitivity near the threshold as shown in Fig. 2 (the larger  $\gamma_i$ , the closest  $u_i$  is to zero near the threshold,  $i = 1, 2$ ) (Fig. 5, left column, bottom). An

analytical characterization of these phenomena is left for future work. Parameters for these simulations are listed in Table II.

2) *Stability properties of the closed loop system:* We just showed that the molecular controller can be tuned so that the closed loop system has a single equilibrium, which can be found numerically as the unique intersection of the equilibrium conditions. Naturally, stability of the equilibrium depends on the eigenvalues of the Jacobian matrix (30) evaluated at such equilibrium. Applying Gershgorin's disk theorem to the columns of Jacobian (30), we can find the following sufficient conditions for stability:  $f_1 < 1$ ,  $f_2 < 1/3$ ,  $\hat{\beta}_1 < 1$ ,  $\hat{\beta}_2 < 1$ . These conditions, however, are just sufficient and not necessary, so they may not be useful in practice. In fact, the system may be stable also when  $f_1$  and  $f_2$  are larger, when  $\hat{\beta}_1$  and  $\hat{\beta}_2$  are suitably chosen; and we are particularly interested in the values of  $\hat{\beta}_i$  that can stabilize the system in this case. In search of tighter conditions, we examined the characteristic polynomial of the Jacobian (30) and applied the Routh Criterion (see Appendix); the inequalities obtained from the Routh table suggest that stability is guaranteed in a limited range of  $\hat{\beta}_i$  (instability can occur if they are too low or too high).

With numerical simulations we examined the behavior of the closed loop system for values of  $\hat{\beta}_i$  up to 10-fold the nominal values listed in Table II (the nominal values were chosen to guarantee a single equilibrium in closed loop). These simulations indicate that trajectories converge to the equilibrium in the entire range of values of  $\hat{\beta}_i$  we considered, as shown in Figs. 4 B and 5. However, for large values of  $\hat{\beta}_i$ ,  $\hat{y}_1(t)$  presents a significant overshoot, which persists even when  $\hat{\gamma}_i$  are increased (we recall that a large value of  $\hat{\gamma}_i$  helps reduce the distance between the equilibrium of the closed loop system and the unstable equilibrium of the toggle switch in isolation, when  $\hat{\beta}_i$  are too large).

Although not exact, our analysis indicates that stability of the closed loop system is robust to controller parameter variations when a single equilibrium is present.

TABLE II

NOMINAL SIMULATION PARAMETERS OF THE CONTROLLED SYSTEM.

Parameter	Description	Value	Other studies
$\beta_1, \beta_2$ (/s)	Production	$1.16 \cdot 10^{-4}$	$2.710^{-4} - 1$ [17], [18] [19], [20]
$\alpha_1, \alpha_2$ (M/s)	Maximal production	$3.85 \cdot 10^{-10}$	$2.81^{-11} - 2.81^{-8}$ [21], [22]
$\theta$ (M/s)	Production	$5.776 \cdot 10^{-10}$	
$\gamma_1, \gamma_2$ (/M/s)	Titration	$2.91 \cdot 10^4$	$10^4 - 10^6$ [23], [24]
$\phi$ (/s)	Degradation	$3.85 \cdot 10^{-4}$	$10^{-4} - 10^{-3}$ [25].
$\kappa_1, \kappa_2$ (nM)		250	
$n$		2	

## IV. NUMERICAL SIMULATIONS

The ODE models described in this paper were integrated using MATLAB's `ode23s` routine, using the nominal parameters listed in Table II. Individual parameters were varied as explained in each simulation figure, leaving all other parameters fixed and equal to their nominal value. Characteristic polynomials and the coefficients of Routh tables were computed with the support of Wolfram Mathematica.

## V. DISCUSSION

The recent efforts toward the constructions of molecular controllers will enable us to engineer robust molecular systems with diverse applications in biotechnology. Here we have highlighted that sequestration-based controllers can be used to stabilize a bistable network in a neighborhood of its unstable equilibrium. The dynamic behavior of bistable switches can be controlled with alternative approaches; an *in silico* controller regulating inducer concentrations can be used to commit a bistable gene network to a particular stable state or to induce switching between steady states [26], [27], [28]. Theoretical analysis has been dedicated to the problem of toggling a bistable system using *in silico* generated pulsed inputs [29]. Our study provides a *molecular circuit* approach to control bistability, in which additional species are used to build a feedback loop around the bistable process. As many experimental efforts are being dedicated to characterizing similar controllers [11], [12], [7], [6], it may be possible to implement the controller suggested here to reshape the equilibrium landscape of complex bistable networks.

## APPENDIX

*Evaluation of the characteristic polynomial of the closed loop Jacobian matrix* The characteristic polynomial of the closed loop system Jacobian matrix (30) is below, in which variable  $\hat{s} = s + 1$ :

$$P_J(\hat{s}) = \hat{s}^2(\hat{s} + T_1)(\hat{s} + T_2)(\hat{s}^2 - F) + D_1 Q_1 \hat{\beta}_1 + D_2 Q_2 \hat{\beta}_2$$

where  $T_1 = \hat{\gamma}_1(\tilde{x}_1 + \tilde{u}_1)$ ,  $T_2 = \hat{\gamma}_2(\tilde{x}_2 + \tilde{u}_2)$ ,  $F = f_1 f_2$ , where  $f_1$  and  $f_2$  are defined at expression (30). We also define  $D_1 = f_2$ ,  $D_2 = f_1 f_2 \hat{\gamma}_2 \tilde{u}_2$ ,  $Q_1 = \hat{s}^2(\hat{s} + C_1)(\hat{s} + T_2)$ , where  $C_1 = \hat{\gamma}_1 \tilde{u}_1$ , and  $Q_2 = \hat{s}(\hat{s} + T_1)$ . We can expand  $P_J(\hat{s})$  and we obtain:

$$P_J(\hat{s}) = \hat{s} \sum_{i=1}^6 a_i \hat{s}^{i-1} \quad (31)$$

where

$$\begin{aligned} a_6 &= 1 \\ a_5 &= T_1 + T_2 \\ a_4 &= T_1 T_2 + D_1 \hat{\beta}_1 - F \\ a_3 &= T_2(D_1 \hat{\beta}_1 - F) + C_1 D_1 \hat{\beta}_1 - F T_1 \\ a_2 &= D_2 \hat{\beta}_2 + T_2(C_1 D_1 \hat{\beta}_1 - F T_1) \\ a_1 &= D_2 \hat{\beta}_2 T_1 \end{aligned}$$

To determine whether the Jacobian admits eigenvalues with positive real part, we build the Routh table shown in

$$J = \begin{bmatrix} -1 & -f_1 & \hat{\beta}_1 & 0 & 0 & 0 \\ -f_2 & -1 & 0 & 0 & \hat{\beta}_2 & 0 \\ -f_2 & 0 & -\hat{\gamma}_1 \tilde{x}_1 - 1 & -\hat{\gamma}_1 \tilde{u}_1 & 0 & 0 \\ 0 & 0 & -\hat{\gamma}_1 \tilde{x}_1 & -\hat{\gamma}_1 \tilde{u}_1 - 1 & 0 & 0 \\ 0 & 0 & 0 & 0 & -\hat{\gamma}_2 \tilde{x}_2 - 1 & -\hat{\gamma}_2 \tilde{u}_2 \\ -f_2 & 0 & 0 & 0 & -\hat{\gamma}_2 \tilde{x}_2 & -\hat{\gamma}_2 \tilde{u}_2 - 1 \end{bmatrix} \quad f_1 = \frac{\hat{\alpha}_1 n \tilde{y}_2^{n-1}}{(\tilde{y}_2^n + 1)^2}, \quad f_2 = \frac{\hat{\alpha}_2 n \tilde{y}_1^{n-1}}{(\tilde{y}_1^n + 1)^2} \quad (30)$$

TABLE III

ROUTH TABLE FOR THE CHARACTERISTIC POLYNOMIAL (31)

5	$a_6 > 0$	$a_4$	$a_2$
4	$a_5 > 0$	$a_3$	$a_1 > 0$
3	$b_1 > 0$	$b_2$	0
2	$c_1$	$a_1 > 0$	0
1	$d_1$	0	0
0	$a_1 > 0$	0	0

Table III, in which the following coefficients were computed and examined using Wolfram Mathematica:

$$b_1 = \frac{a_5 a_4 - a_3 a_6}{a_5} > 0, \quad b_2 = \frac{a_5 a_2 - a_1 a_6}{a_5}$$

$$c_1 = \frac{a_3 b_1 - a_5 b_2}{b_1}, \quad d_1 = \frac{c_1 b_2 - a_1 b_1}{c_1}.$$

To guarantee that no eigenvalue has a positive real part, both  $c_1$  and  $d_1$  should be positive. Because we focus on the role of the controller parameters  $\hat{\beta}_i$ , we rewrite coefficients  $c_1$  and  $d_1$  isolating  $\hat{\beta}_i$ , and we find that  $c_1$  and  $d_1$  are second order polynomials of  $\hat{\beta}_1$  and  $\hat{\beta}_2$ . Some of the coefficients of these polynomials are sign definite, others are not. Specifically:  $c_1 = \hat{\beta}_1^2 \pm \xi_1 \hat{\beta}_1 - \xi_2 \hat{\beta}_2$ , and  $d_1 = \hat{\beta}_2^2 - \xi_3 \hat{\beta}_2 - \xi_4$ , where  $\xi_3 = \zeta_1(\hat{\beta}_1^2 \pm \zeta_2 \hat{\beta}_1 \pm \zeta_3)$  and  $\xi_4 = \zeta_4 \hat{\beta}_1(\hat{\beta}_1^2 \pm \zeta_5 \hat{\beta}_1 \pm \zeta_6)$ . We use the  $\pm$  notation to emphasize that the following term could be positive or negative. Because  $c_1$  has a positive dominant term, then for large  $\hat{\beta}_1$ ,  $c_1$  can become positive. However, when  $\hat{\beta}_1$  is larger enough to make  $c_1$  positive,  $d_1$  could become negative. When  $\hat{\beta}_2$  is large, it can make  $d_1$  positive, but also make  $c_1$  negative. This suggest that there is a bounded range of values of  $\hat{\beta}_i$ ,  $i = 1, 2$  for which  $c_1$  and  $d_1$  are positive and the equilibrium is stable.

## REFERENCES

- [1] G. Craciun, Y. Tang, and M. Feinberg, "Understanding bistability in complex enzyme-driven reaction networks," *Proceedings of the National Academy of Sciences*, vol. 103, no. 23, pp. 8697–8702, 2006.
- [2] J. R. Pomeroy, E. D. Sontag, and J. E. Ferrell Jr, "Building a cell cycle oscillator: hysteresis and bistability in the activation of *cdc2*," *Nature cell biology*, vol. 5, no. 4, p. 346, 2003.
- [3] W. Xiong and J. E. Ferrell Jr, "A positive-feedback-based bistable memory module that governs a cell fate decision," *Nature*, vol. 426, no. 6965, p. 460, 2003.
- [4] E. S. Wright and K. H. Vetsigian, "Inhibitory interactions promote frequent bistability among competing bacteria," *Nature communications*, vol. 7, p. 11274, 2016.
- [5] B. C. Mulukutla, A. Yongky, P. Daoutidis, and W.-S. Hu, "Bistability in glycolysis pathway as a physiological switch in energy metabolism," *PloS one*, vol. 9, no. 6, p. e98756, 2014.
- [6] H.-H. Huang, Y. Qian, and D. Del Vecchio, "A quasi-integral controller for adaptation of genetic modules to variable ribosome demand," *Nature communications*, vol. 9, no. 1, p. 5415, 2018.
- [7] G. Lillacci, Y. Benenson, and M. Khammash, "Synthetic control systems for high performance gene expression in mammalian cells," *Nucleic acids research*, vol. 46, no. 18, pp. 9855–9863, 2018.
- [8] T. S. Gardner, C. R. Cantor, and J. J. Collins, "Construction of a genetic toggle switch in *Escherichia coli*," *Nature*, vol. 403, no. 6767, p. 339, 2000.
- [9] C. C. Samaniego and E. Franco, "An ultrasensitive motif for robust closed loop control of biomolecular systems," in *2017 IEEE 56th Annual Conference on Decision and Control (CDC)*. IEEE, 2017, pp. 5334–5340.
- [10] C. C. Samaniego, G. Giordano, and E. Franco, "Practical differentiation using ultrasensitive molecular circuits," in *2019 18th European Control Conference (ECC)*. IEEE, 2019, pp. 692–697.
- [11] E. Franco, G. Giordano, P.-O. Forsberg, and R. M. Murray, "Negative autoregulation matches production and demand in synthetic transcriptional networks," *ACS synthetic biology*, vol. 3, no. 8, pp. 589–599, 2014.
- [12] V. Hsiao, E. L. De Los Santos, W. R. Whitaker, J. E. Dueber, and R. M. Murray, "Design and implementation of a biomolecular concentration tracker," *ACS synthetic biology*, vol. 4, no. 2, pp. 150–161, 2014.
- [13] C. Briat, A. Gupta, and M. Khammash, "Antithetic integral feedback ensures robust perfect adaptation in noisy biomolecular networks," *Cell systems*, vol. 2, no. 1, pp. 15–26, 2016.
- [14] N. E. Buchler and F. R. Cross, "Protein sequestration generates a flexible ultrasensitive response in a genetic network," *Molecular systems biology*, vol. 5, no. 1, p. 272, 2009.
- [15] C. C. Samaniego, E. Franco, and G. Giordano, "Design and analysis of a biomolecular positive-feedback oscillator," in *2018 IEEE Conference on Decision and Control (CDC)*. IEEE, 2018, pp. 1083–1088.
- [16] C. Cuba Samaniego and E. Franco, "A robust molecular network motif for period-doubling devices," *ACS synthetic biology*, vol. 7, no. 1, pp. 75–85, 2017.
- [17] R. Hussein and H. N. Lim, "Direct comparison of small RNA and transcription factor signaling," *Nucleic acids research*, vol. 40, no. 15, pp. 7269–7279, 2012.
- [18] R. Milo and R. Phillips, *Cell biology by the numbers*. Garland Science, 2015.
- [19] U. Vogel and K. F. Jensen, "The RNA chain elongation rate in *Escherichia coli* depends on the growth rate," *Journal of Bacteriology*, vol. 176, no. 10, pp. 2807–2813, 1994.
- [20] H. Chen, K. Shiroguchi, H. Ge, and X. S. Xie, "Genome-wide study of mRNA degradation and transcript elongation in *Escherichia coli*," *Molecular systems biology*, vol. 11, no. 1, p. 781, 2015.
- [21] Y. Qian, H.-H. Huang, J. I. Jimenez, and D. Del Vecchio, "Resource competition shapes the response of genetic circuits," *ACS synthetic biology*, vol. 6, no. 7, pp. 1263–1272, 2017.
- [22] S. Basu, Y. Gerchman, C. H. Collins, F. H. Arnold, and R. Weiss, "A synthetic multicellular system for programmed pattern formation," *Nature*, vol. 434, no. 7037, p. 1130, 2005.
- [23] J. Kim, K. S. White, and E. Winfree, "Construction of an *in vitro* bistable circuit from synthetic transcriptional switches," *Molecular systems biology*, vol. 2, no. 1, p. 68, 2006.
- [24] D. Y. Zhang, A. J. Turberfield, B. Yurke, and E. Winfree, "Engineering entropy-driven reactions and networks catalyzed by DNA," *Science*, vol. 318, no. 5853, pp. 1121–1125, 2007.
- [25] J. Kim, I. Khetarpal, S. Sen, and R. M. Murray, "Synthetic circuit for exact adaptation and fold-change detection," *Nucleic acids research*, p. gku233, 2014.
- [26] J.-B. Lugagne, S. S. Carrillo, M. Kirch, A. Köhler, G. Batt, and P. Hersen, "Balancing a genetic toggle switch by real-time feedback control and periodic forcing," *Nature communications*, vol. 8, no. 1, p. 1671, 2017.
- [27] D. Fiore, A. Guarino, and M. di Bernardo, "Analysis and control of genetic toggle switches subject to periodic multi-input stimulation," *IEEE control systems letters*, vol. 3, no. 2, pp. 278–283, 2019.
- [28] A. Guarino, D. Fiore, and M. di Bernardo, "In-silico feedback control of a mimo synthetic toggle switch via pulse-width modulation," *arXiv preprint arXiv:1811.06263*, 2018.
- [29] A. Sootla, D. Oyarzún, D. Angeli, and G.-B. Stan, "Shaping pulses to control bistable systems: Analysis, computation and counterexamples," *Automatica*, vol. 63, pp. 254–264, 2016.